NUMERICAL STUDY OF INDENTATION TESTING IN SUPERFICIAL COATINGS

Avelino Manuel da Silva Dias, avelino@ufsj.edu.br
Mechanical Department – Federal University of São João Del-Rei
Frei Orlando Square, 170 – São João Del-Rei – MG
36307-352

Geralda Cristina Durães de Godoy, gcgodoy@demet.ufmg.br
Paulo José Modenesi, modenesi@demet.ufmg.br
Sara Del Vecchio, saradvec@yahoo.com.br
Engineering School – Federal University of Minas Gerais
Espírito Santo Lane, 35 – Belo Horizonte – MG

Abstract. *The aim of this work was to simulate the indentation testing behaviour of a rigid ball indenter on a coating/substrate system by the finite element method. Indentation testing has been used for a long time to determinate the superficial hardness of different materials. Recently, a number of researchers have developed new techniques based on this testing to evaluate different mechanical properties of materials including toughness and the Young modulus. This technique has also been used to characterise and analyse superficial coatings. However, there are still limitations to analyze the coating/substrate system behaviour during indentation testing. To help to reduce those limitations, the present work uses the finite element technique to simulate stress and strain fields during the indentation testing cycle. A commercial finite element code which has been considered as a promising tool for non linear problems and fracture process was used. The numerical results for the stress and strain fields focused mainly in the indenter contact region and for coating/substrate interface were calculated during the indentation cycle. Furthermore, through the use of the maximum principal stress criterion, details of the failure mechanism that occurs on coating system were evaluated.*

Keywords: Finite Element, Nano-indentation, Thin Films, Contact.

1. INTRODUCTION

Nowadays, nano-indentation testings have been used as a potential tool to evaluate mechanical characteristics of materials including, for example, the Young modulus (E), the Poisson coefficient (ν) and also the entire elastic-plastic stress *versus* strain curve under compression (Zeng and Chiu, 2001; Lee *et al.*, 2005). However, the implementation of this indentation technique to obtain different mechanical properties does still bring many doubts to the scientific community. These doubts are particularly stronger when the testing procedure is used to evaluate the mechanical behaviour of hard thin films applied over soft metal substrates. The limitations of this testing procedure have triggered, the use of numerical techniques to simulate it, including the calculation of the stress and strain fields during the indentation cycle, to allow a more reliable interpretation of it.

In the last few years, a great volume of research work has been developed to evaluate the behaviour of different material classes during indentation testing by use of numerical techniques (Sun *et al.*, 1995; Souza *et al.*, 2001; Carpinteri *et al.*, 2004; Piana *et al.*, 2005; Antunes *et al.*, 2006; Dias *et al.*, 2006; Vanimisetti and Narasimhan, 2006). On the other hand, the use of numerical techniques to study the indention testing on thin superficial coatings has also presented several problems mainly associated to the difficulty to characterize these coatings, to establish and implement failure criteria, and, mainly, to obtain reliable mechanical properties of the coating/substrate system. Furthermore, computational limitations are also indicated as difficulties (Sun *et al.*, 1995; Vanimisetti and Narasimhan, 2006).

Plastic deformation is a major concern in the design and performance of engineering components. Failure of a hard coating/soft substrate system under many tribological situations is seldom caused by conventional wear but by debonding of the coating from the substrate (adhesive failure), or fracture of the coating (cohesive failure), or even by subsurface fracture (substrate failure). Accordingly, it is imperative to determine the spatial distribution of the plastic strain and the initiation and development of the plastic zone, so as to have a better understanding of the mechanisms of surface and subsurface wear involving localized plastic flow (Sun *et al.*, 1995).

In an attempt to comprehend the mode of deformation of a surface coating during the indentation cycle with a spherical indenter, Vanimisetti and Narasimhan (2006) published results from a numerical analysis of the test of a thin hard film deposited on a soft substrate. The authors analysed the film stress field distribution and identified a transition of this stress field during the testing, which varied from a contact stress field to flexure stress in the beginning of the testing. Moreover, depending on the indentation depth, the film stress field behaved as membrane stress with tension stresses on both circumferential and radial directions. The authors evaluated the influence of the system (coating and

substrate) yield strength and the presence of residual stresses on the indentation response. Finally, they present an initial study of fracture process that occurs in this system during the indentation testing.

The proposed simulations of this work were performed using the Finite Element Method (FEM) on a commercial solver (MARC™, 2005). This methodology has been greatly used to simulate and solve many non-linear problems in different areas like structural instability, dynamic, fluid and electromagnetic systems, and mechanical forming and fracture process (Dias, 2004). The principal aim of this work was to evaluate the contact stress and strain fields during the indention testing with rigid spherical indenter on coating/substrate systems with different penetration depths. It were analysed four monolayer systems produced by plasma deposition (PADVD), recovered of Chromium Nitrate (CrN) with different thickness on two metal substrates.

2. METHODOLOGY

The indentation testing consist of a penetration an indenter, which may, in most cases, considered a rigid body, on the surface of a sample of the analysed material (Souza, 2000). For the simulation of this test with a spherical indenter, the symmetry of the problem was considered and two dimensional axis-symmetric elements were used in the model, which greatly reduced the complexity and computational effort need to analyze the problem.

The numerical simulation the indentation cycle (including both loading and unloading steps) presented in this work, a prescribed displacement scheme was used to guarantee a better control in the beginning and during all the indentation cycle (Dias, 2004). This procedure is consistent with experimental nano-indentation testing, since the indenter displacement is applied with a small penetration speed and the behaviour of the load versus displacement is obtained by the load sensor installed on the indenter table. Besides this numerical control, the simulation was developed in two phases, one related to the indenter coming down, followed by its coming up, and the completing the cycle (Dias *et al.*, 2006). The Pile-up and sinking-in surface displacements, which can occur during the testing, were not taken into consideration in this work. Likewise, the friction coefficient between the indenter and the testing sample was considered to be zero, because there is some evidence that this friction do not interfere with the numerical results (Lee *et al.*, 2005; Dias *et al.*, 2006). In improve the results of the stress field distribution in the indenter contact region and in the coating and substrate interface, a more refined mesh was used in these regions, Fig. 1.

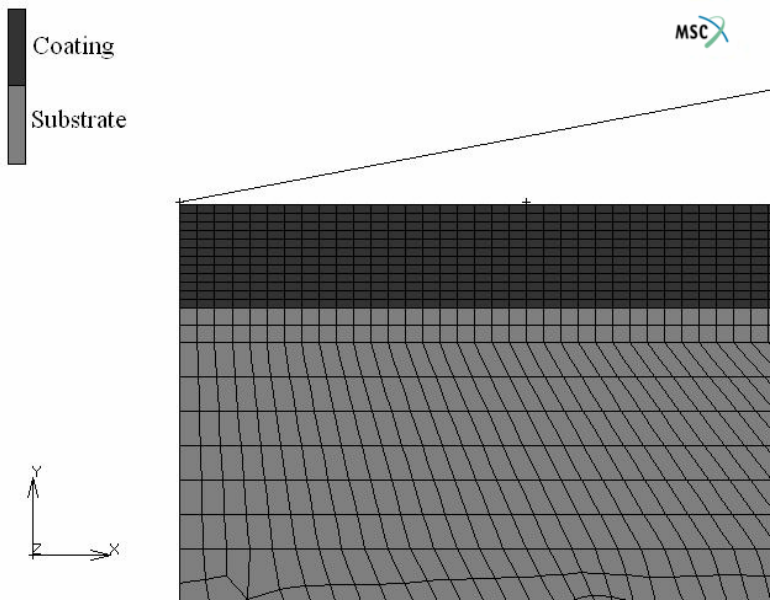

Figure 1. Detail of the numerical model mesh close to the contact area.

In present analysis, the spherical indenter was modelled as a rigid semicircular shell, with three different diameters which penetrates in the sample of the studied systems. It was considered that a perfect adherence exists between the coating and the substrate. The boundary conditions included a displacement restriction that was imposed to the base of the sample and radial displacement restriction to the nodes localized in the axis of symmetry (Sun *et al.*, 1995). During the simulation, two hundreds increments were used to represent the penetration of the indenter and one hundred to model its removal from the sample, completing the indentation cycle.

Different systems, composed by monolayer coatings of CrN, with two different thicknesses (t), and two metal substrates (SAE 1045 carbon steel and AISI 301 stainless steel) were simulated. For the system with thicker film (t = 15μm), 1036 isoperimetric axis-symmetric elements with eight nodes were used, being 460 elements were used to

represent the film and the remainder for the substrate. On the other hand, for the sample with smaller thickness film (t = 5μm), it was only 806 elements with eight nodes.

The adopted penetration depth ($h_{máx}$) was 1,5 μm for the systems with smaller thickness and varied from 2,5 μm to 7,5 μm for the system with bigger thickness. Those $h_{máx}$ values were based on results from tests performed in an instrumented ultra-microhardness equipment (Mancosu, 2005).

Table 1 shows the mechanical properties of the materials that were used in this work values founded in the specialized literature. Both the coating and the substrate materials were considered isotropic and homogeneous. It was adopted following models for the elastic-plastic behaviour of the system were adopted: the CrN film was considered as perfectly plastic (Sun *et al.*, 1995); the stainless steel (AISI 301) was represented through an elastic-plastic flow curve (Dias, 2004); and the carbon steel (SAE 1045) was represented by a stress *versus* strain curve obtained on the finite element solver library (MARC™, 2005).

Table 1. Mechanical properties of the materials used in this work (Mancosu, 2005; Shigley, 1986)

Material	Young Modulus (E)	Poisson Coefficient (ν)	Yield Strength (σ_y)
Coating (CrN)	380 GPa	0,22	4000 MPa
Substrate (AISI 301)	195 GPa	0,3	1900 MPa
Substrate (SAE 1045)	217 GPa	0,3	400 MPa

3. TESTING THE MODEL

The validity of the numerical model was tested by comparing the FE results for the contact between the uncoated system and the rigid ball with the results of analytical Hertz solution, Eq. (1), for a rigid sphere and a semi-infinite plane plate (Shigley, 1986). In this expression, a was the contact area radius, F was the force and R was the radius of the indenter. In this procedure, a linear elastic analysis was adopted.

$$a = \sqrt[3]{\frac{3FR}{E^*}} \tag{1}$$

$$E^* = \frac{E}{\left(1-\nu^2\right)} \tag{2}$$

Applying Eq. (1) and Eq. (2) to the contact between a spherical indenter with a radius of 100 μm and a metallic substrate (E = 195 GPa and ν = 0,3), it was obtained the analytical value for the elastic contact radius (a), which presented a difference of 5,3 % when compared to the value obtained numerically. This procedure demonstrated that the numerical model was able to represent well the contact between the indenter and the sample and the stress gradient in the contact region.

4. RESULTS AND DISCUSSIONS

Table 2 compares the indentation force obtained for different systems by the simulation analysis. As the simulation was performed by imposing a prescribed displacement to the indenter ($h_{máx}$), different indentation forces were obtained according to the mechanical properties of each system. The results indicate that, for similar systems, those with a thicker coating required a larger force during indentation. On the other hand, when different systems were compared, those with a stronger substrate needed a larger indentation force. Also, as expected, the penetration force increased if the penetration depth was increased for the same system.

The calibration procedure of the numerical model and the first results presented above indicated qualitatively that the developed simulation can represent some aspects of the global behaviour of nano-indentation testing of Chromium Nitrate monolayer coating over two different metallic substrates.

Figure 2 presents numerical results of equivalent plastic strain during tests with a 1 mm diameter indenter and a depth of penetration of 5 μm. The simulated system was a 15 μm-thick coating of CrN on AISI 301 stainless steel (CrN-AISI 301). In this simulation, the depth of penetration represented 16.7% of the coating thickness, and, depending on the contact area between the indenter and the sample, there was a gradient of bending stresses during the test. The data were obtained from four nodes of the model. Two nodes were in the coating, one (node 4) was located under the indenter in the half thickness of the coating, and the second (node 907) in the interface between the coating and the substrate. The other two nodes (9 and 909) were located in the substrate, both close to the coating/substrate interface. Figure 2 illustrates that the plastic zone initiated both in the coating and also in the substrate near the interface. Once it

is formed, the plastic zone develops more intensely near the interface. According to Sun *et al*. (1995), when plastic zones are formed in both coating and substrate during the indentation cycle, the film thickness and its mechanical strength are not sufficient to protect the system against delamination. The numerical result present in Fig. 2 suggests that this may be the case for the system considered (CrN–AISI 301 with h_m of 15 μm).

Table 2. Calculated indenter force for different systems.

System	Diameter indenter	Thickness of film	Indentation depth	Ratio $t \times h_m$	Indenter force
CrN-SAE 1045	200 μm	5 μm	1.5 μm	0.300	30.1 N
		15 μm	2.5 μm	0.167	51.8 N
	100 μm	15 μm	2.5 μm	0.167	47.3 N
			5.0 μm	0.333	60.3 N
			7.5 μm	0.500	69.2 N
	1 mm	15 μm	2.5 μm	0.167	52.9 N
			5.0 μm	0.333	103.8 N
			7.5 μm	0.5	123.2 N
CrN-AISI 301	200μm	5 μm	1.5 μm	0.300	58.8 N
		15 μm	2.5 μm	0.167	102.5 N
	100 μm	15 μm	2.5 μm	0.167	87.6 N
			5.0 μm	0.333	123.9 N
			7.5 μm	0.500	139.7 N
	1 mm	15 μm	2.5 μm	0.167	116.7 N
			5.0 μm	0.333	209.8 N
			7.5 μm	0.500	248.2 N

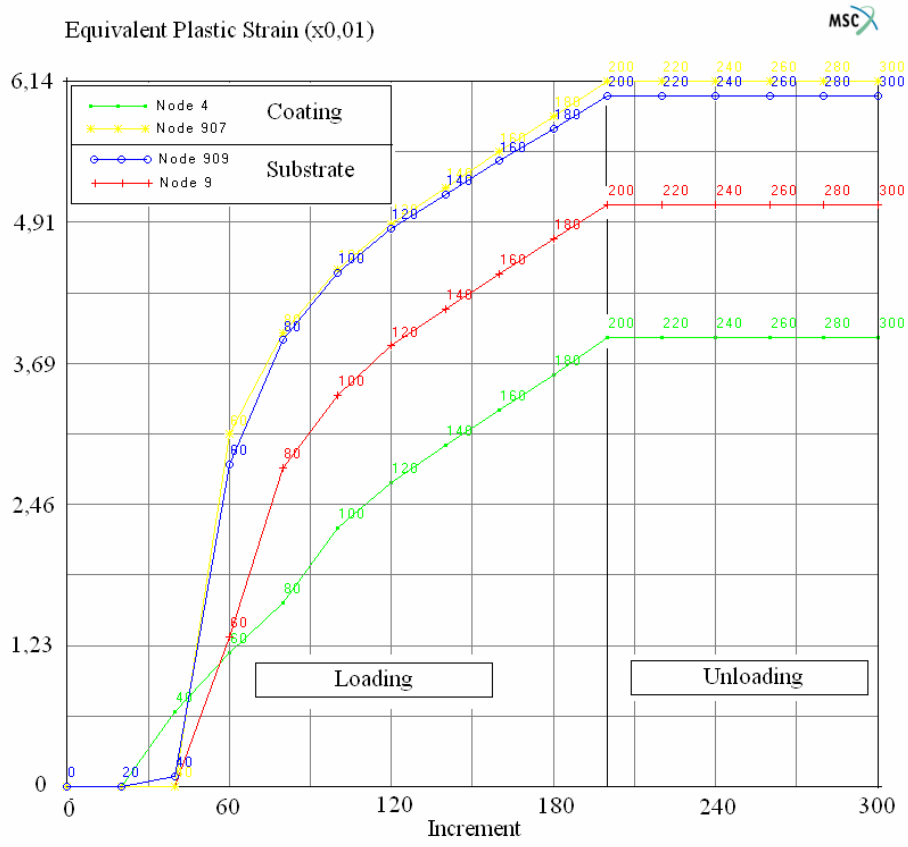

Figure 2. Numerical evaluation of equivalent plastic strain during indentation cycle

When the results of Fig. 2 are compared to those obtained for thinner coatings, it can be seen that systems with ticker coatings present smaller plastic deformation fields. Also, the stress gradient over the interface was larger for systems where a larger penetration depth to coating thickness ratio was used (Dias *et al.*, 2007).

Figure 3 presents the normal stress distribution predicted by the numerical simulation during indentation of a CrN-SAE 1045 steel (coating thickness of 15 μm). A 1 mm diameter indenter and a depth of penetration of 5 μm were considered. The three nodes considered in Fig. 3 were located on the coating. One was located close to the coating surface (node 2), the second was in the middle of the coating (node 4), and the third next to the coating/substrate interface (node 6). A change in the stress gradient behaviour can be noticed during the indentation cycle. Initially, the stress field resulted from the contact between the indenter and the sample. Later, it became a bending field and, by the end of the loading cycle, membrane stress field are formed. By the end of the test, a tension residual stress field is formed. Similar changes in stress field are reported by Vanimisetti and Narasimhan (2006), who related this behaviour to the depth of penetration and to the contact area ratio. Similar behaviour was observed on the other simulated systems. It was more intense in thin coating systems and for higher penetration depths.

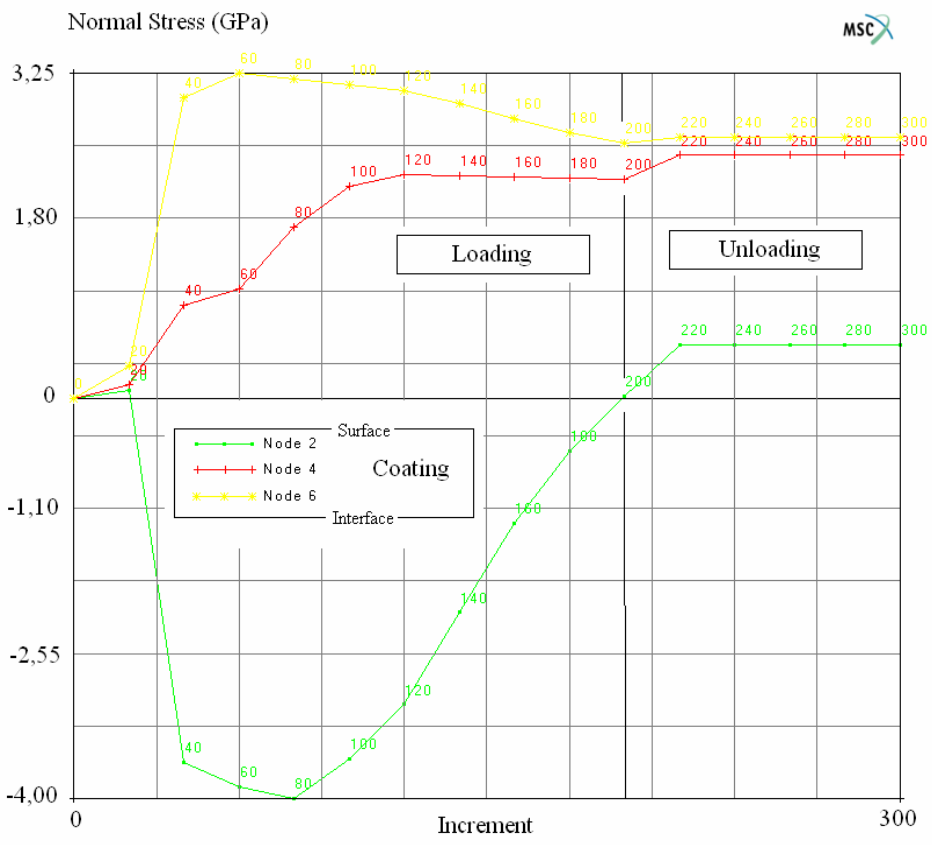

Figure 3. Numerical evaluation of normal stress in coating during indentation testing

Circumferential cracks around the indenter are commonly formed during indentation testing of hard coatings with spherical indenters. Cracks of this kind can be observed in Fig. 4 for a duplex thin film of CrAlN deposited by PADVD on a stainless steel nitrated by plasma (Mancosu, 2005).

Figure 5 shows the numerically predicted distribution of maximum principal stress on a radial plane for an indentation test of the CrN-SAE 1045 steel system with an $h_{máx}$ of 2,5 μm. Considering the CrN film as a brittle material and using Rankine theory as a failure criterion, it is possible to identify two critical regions, one on the surface of the specimen and close to the indentation, and another near the interface between the substrate and the film. In both regions the calculated stress reach values close to the yield stress of the coating, Tab. 1. Those regions were also found in the other systems that were simulated in the present work. To better emphasize this aspect, the behaviour during the indentation cycle of points inside these regions was studied.

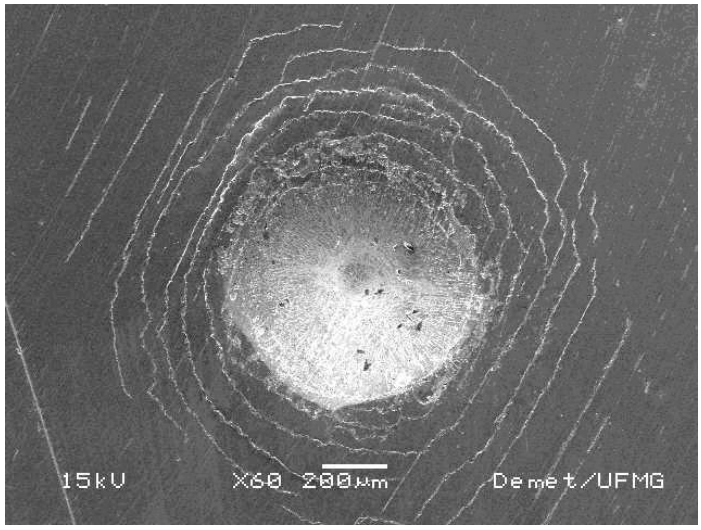

Figure 4. Circular cracks around impression of spherical indenter (Mancosu, 2005)

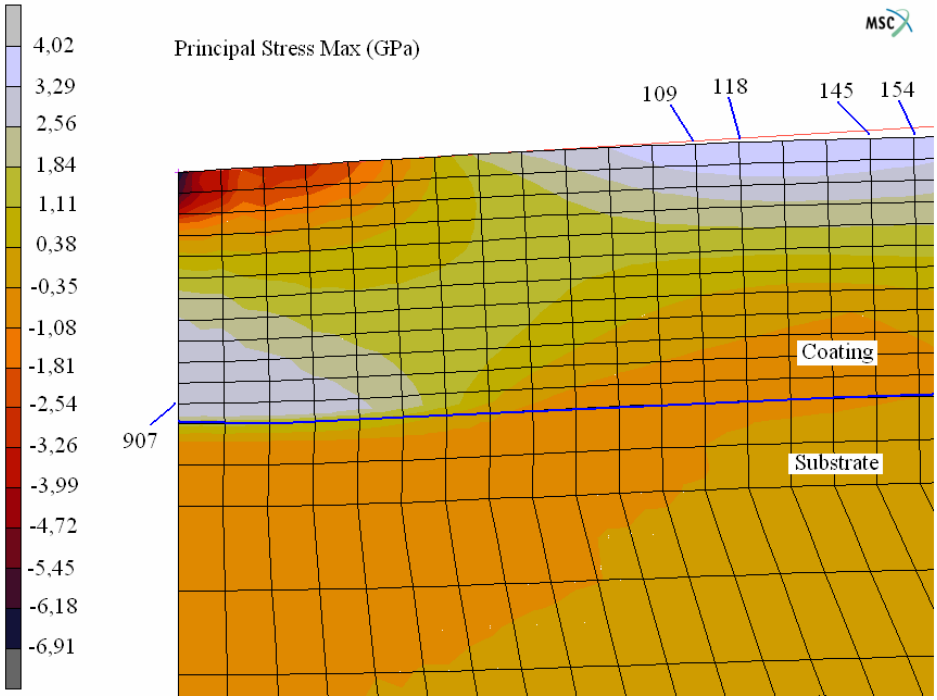

Figure 5. Numerical distributions of the maximum principal stress in the contact area

Figure 6 presents the evolution of the maximum principal stress during an indentation cycle of the CrN-AISI 301 (coating thickness of 15 µm) system. It can be seen that the stress in nodes close to the film surface reach 3,67 GPa. This value is very close to yield strength of the coating material under compression, and, therefore, critical to this material under traction. This result is supported by experimental results from nano-indentation tests. The calculated maximum principal stress for a node (907) situated close to coating/substrate interface reached 1,80 GPa and that also indicates that this may be considered as a critical region of the system during the indentation cycle.

Figure 7 also shows the evolution of the maximum principal stress during the indentation cycle of the CrN-SAE 1045 system. Again, it can be observed that, for nodes close to the film surface, this stress reaches values close to the yield strength of the film material (4,02 GPa). The same holds for a node located close to the substrate-film interface that reaches a maximum principal stress of 3,40 GPa and remains under traction during all the indentation cycle. When the plot of Fig. 7 was compared to the previous one, it could be observed that the film of the CrN-SAE 1045 system presents a larger stress gradient as expected for a system with a less strong substrate. This observation also agrees with results from the literature.

Finally, the stress levels found in these notes also suggest the possibility of delamination in this system.

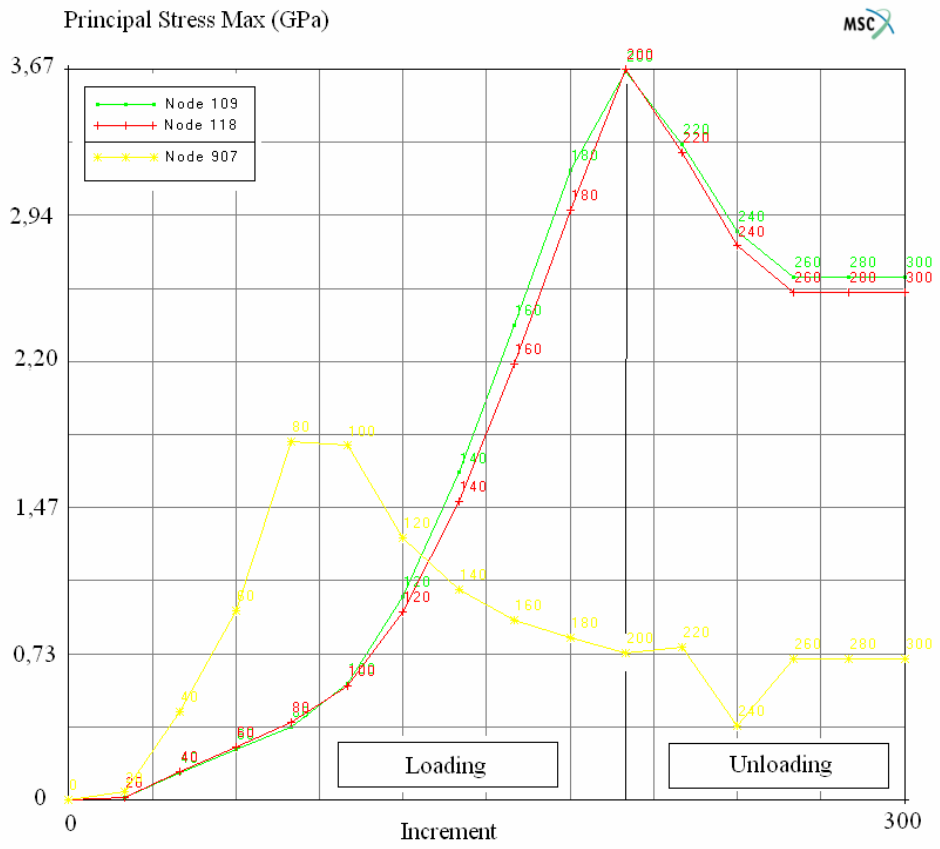

Figure 6. Numerical evolution of highest principal stress during indention testing in CrN–AISI 301 system

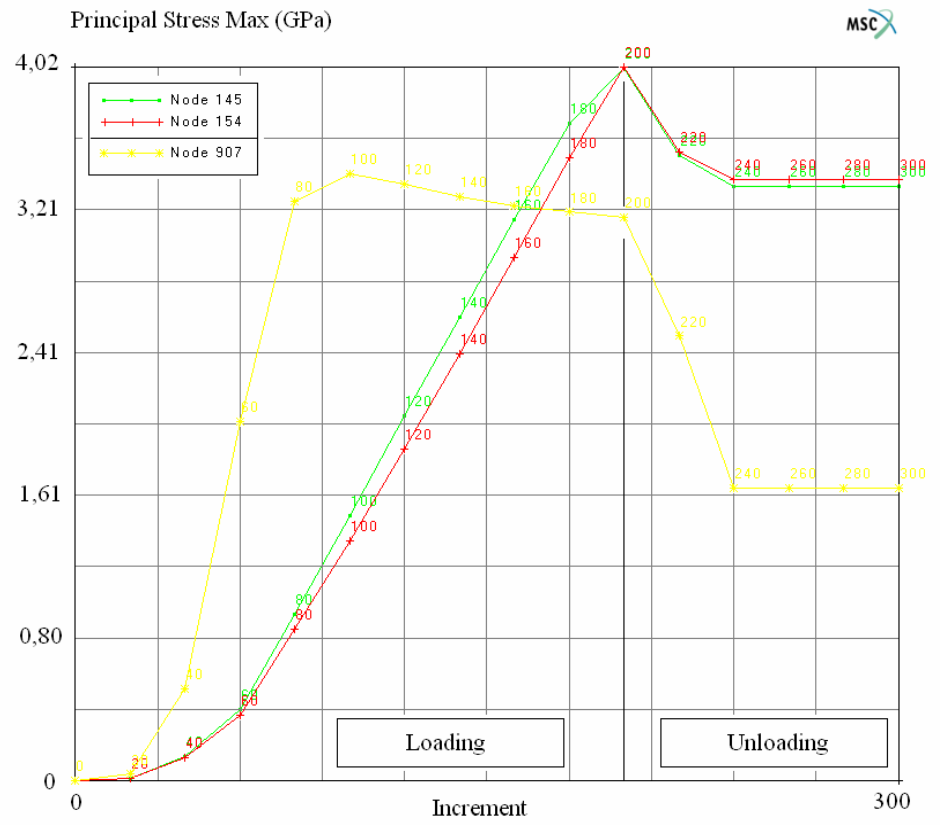

Figure 7. Numerical evolution of highest principal stress during indention testing in CrN–SAE 1045 system

5. CONCLUSIONS

Based on the numerical results of the nano-indentation essay with spherical indenter of coating/substrate systems by finite element method, it was possible to present the following conclusions:

- The numerical model represented adequately the elastic contact between the indenter and the sample when it was compared to results calculated using Hertz solution.
- The global behaviour of some systems was well modelled by the CrN monolayer numerical simulation with different film thickness deposited on two different metallic substrates.
- The calculated stress during the indentation cycle changed from a contact stress field to bending stresses, and then to a membrane stress field during the unloading stage. Two plastic strain fields were formed, one in the substrate and another in the film.
- Using Rankine theory as a failure criterion, it was possible to find regions more prone to cracking. These regions correspond well to experimental results reported from nano-indentation testing with spherical indenter. On the other hand, it was possible to identify the possibility of delamination using the same criterion.
- A deeper evaluation of these results is, however, necessary to characterize more clearly the processes of delamination and fracture in the coating as well as failure in the substrate (subsurface fracture).
- There is also need for more reliable tests to determine the mechanical properties of the coating/substrate conjugate and, consequently, improve the numerical simulations.

6. ACKNOWLEDGEMENTS

This research work was supported by FAPEMIG (Foundation for the Support of Research in the State of Minas Gerais).

7. REFERENCES

Antunes, J. M., Menezes, L. F., Fernandes, J. V., 2006, "Three-dimensional Numerical Simulation of Vickers Indentation Testing", International Journal of Solids and Structures, 43, pp. 784-806. <www.elsevier.com/locate/ijsolstr>

Carpinteri, A., Chiaia, B., Invernizzi, S., 2004, "Numerical Analysis of Indentation Fracture in Quasi-brittle Materials", Engineering Fracture Mechanics, 71, pp. 567-577. <www.elsevier.com/locate/engfracmech>

Dias, A. M. S., 2004, "Análise Numérica do Processo de Fratura no Ensaio de Indentação Vickers em uma Liga de WC-Co", Tese de Doutorado, Universidade Federal de Minas Gerais, 200p.

Dias, A. M. S., Modenesi, P. J., Cristina, G. C., 2006, "Computer Simulation of Stress Distribution During Vickers Hardness Testing of WC-6Co", Materials Research, v. 9, n. 1, pp. 73-76. <www.nit.ufscar.br/nit/parcerias/index.htm>

Dias, A. M. S., Modenesi, P. J., Cristina, G. C., 2007, "Estudo do Comportamento de recobrimentos Superficiais através da Análise Numérica do Ensaio de Indentação", Proceedings of Congresso Ibérico de Tribologia, Bilbao, Espanha. (*in press*)

Lee, H., Lee, J. H., Pharr, G. M., 2005, "A Numerical Aproach to Spherical Indentation Techniques for Material Property Evaluation", Journal of the Mechanics and Physics of Solids, 53, pp. 2037-2069. <www.elsevier.com/locate/jmps>

Mancosu, R. D., 2005, "Recobrimento Tribológico Cr-N e Nitretação a Plasma para Melhoria da Resistência à Erosão Cavitacional de um Aço Carbono ABNT 1045: Uma Abordagem Topográfica", Tese de Doutorado, Universidade Federal de Minas Gerais, 335p.

MARC, Msc, 2005, "Volume A: Theory and User Information", Users Manual.

Piana, L. A., Pérez R, E. A., Souza, R. M., Kunrath, A. O., Strohaecker, T. R., 2005, "Numerical and Experimental Analyses on the Indentation of Coated Systems with Substrates with Different Mechanical Properties", Thin Solid Films, 491, pp. 197-203. <www.elsevier.com/locate/tsf>

Shigley, J. E., 1986, "Mechanical Engineering Design", McGraw Hill, 1st Metric Edition, Singapore, 699p.

Souza, S. A., 2000, "Ensaios Mecânicos de Materiais Metálicos: Fundamentos Teóricos e Práticos", Ed. Edgard Blücher LTD, 5th Ed., 286p.

Souza, R. M., Mustoe, G. G. W., Moore, J. J., 2001, "Finite Element Modelling of the Stresses, Fracture and Delamination During the Indentation of Hard Elastic Films on Elastic-Plastic Soft Substrates", Thin Solid Films, 392, pp. 65-74. <www.elsevier.com/locate/tsf>

Sun, Y., Bloyce, A., Bell, T., 1995, "Finite Element Analysis of Plastic Deformation of Various TiN Coating/Substrate Systems under Normal Contact with a Rigid Sphere", Thin Solid Films, 271, pp. 122-131. <www.elsevier.com/locate/tsf>

Vanimisetti, S. K., Narasimhan, R., 2006, "A Numerical Analysis of Spherical Indentation Response of Thin Hard Films on Soft Substrates", International Journal of Solids and Structures, 43, pp. 6180-6193. <www.elsevier.com/locate/ijsolstr>

Zeng, K., Chiu, C., 2001, "An Analysis of Load-Penetration Curves from Instrumented Indentation", Acta Materialia, 49, pp.3539-3551. <www.elsevier.com/locate/actamat>

8. RESPONSIBILITY NOTICE

The authors are the only responsible for the printed material included in this paper.